To appear in The Astrophysical Journal Letters

Dust emission from protostars: the disk and envelope of HH24MMS

Claire J. Chandler[1], David W. Koerner[2], Anneila I. Sargent[3] and Douglas O. S. Wood[1,4]

[1] *National Radio Astronomy Observatory, P.O. Box O, Socorro, NM 87801*

[2] *Jet Propulsion Laboratory, Mail Code 169-506, 4800 Oak Grove Drive, Pasadena, CA 91109*

[3] *Division of Physics, Mathematics, and Astronomy, 105-24, California Institute of Technology, Pasadena, CA 91125*

[4] *Present address: Kodak Scientific Imaging Systems, 4 Science Park, New Haven, CT 06511*

1 Introduction

Circumstellar disks appear to be a natural by-product of star formation. They probably form at a very early stage, reducing angular momentum in the collapsing core and allowing accretion onto the central protostar (cf. Shu et al. 1993). Thermal emission from dust at millimeter and submillimeter wavelengths provides an important means of investigating the structure of circumstellar material surrounding embedded protostars because it is likely to be optically thin, and the radiative transfer is relatively simple compared to the molecular line case. For very deeply embedded sources, the dust emission may comprise two components: one from the disk, and another from an extended envelope. Terebey, Chandler, & André (1993) describe in detail the expected envelope emission.

Investigating the properties of disks can be complicated by a surrounding envelope, which may become optically thick and obscure the disk at far-infrared wavelengths. For dust column densities similar to those in T Tauri disks, the disk emission can be partially optically thick even at λ=1.3 mm (Beckwith et al. 1990). Observations of the circumstellar material at longer wavelengths (e.g., $\lambda \gtrsim$ 3 mm) are therefore essential, where a larger fraction of both the disk and envelope emission is optically thin.

Here we present an investigation of HH24MMS at wavelengths of 3 mm and longer. This cold condensation in the NGC 2068 region of Orion was recently discovered through its 1.3 mm dust emission (Chini et al. 1993). Analysis of the continuum and molecular line emission confirms that HH24MMS is a very young protostar surrounded by an $\sim 5 M_{\odot}$ envelope of cold ($T \lesssim 30$ K) molecular gas (Ward-Thompson et al. 1995; Krügel & Chini 1994). A compact 3,6 cm source at the position of the submillimeter peak has been identified as thermal free-free emission (Bontemps, André, & Ward-Thompson 1995), Our $\lambda \geq 3$ mm measurements constrain the nature of both the submillimeter source and the radio emission.

2 Observations and results

Observations of HH24MMS at 43.3 GHz ($\lambda \approx$ 7 mm) were obtained using the inner 10 antennas of the Very Large Array of the National Radio Astronomy Observatory [1] on 1994 December 7 in the C configuration. Observations at 14.9 GHz (λ = 2 cm) were made on 1995 February 11 using the full array in CnD configuration. For all measurements the total bandwidth was 100 MHz and two circular polarizations were observed. Atmospheric and instrumental phase fluctuations were monitored by observing the quasars 0529+075 at 14.9 GHz, and 0605–085 at 43 GHz. The absolute flux density scales were determined from 3C48 at 14.9 GHz, and 3C48 and 3C286 at 43 GHz. Adopted flux densities, obtained by extrapolating from lower frequencies using the polynomial

[1] The NRAO is operated by Associated Universities, Inc., under cooperative agreement with the National Science Foundation.

form of Baars et al. (1977) with coefficients determined by R. Perley (private communication), are given in Table 1. These could be in error by as much as 20'% and are the most significant source of uncertainty at 43 GHz. Furthermore, both sources are unresolved at 43 GHz and are probably variable, Flux densities measured for the phase calibrators are listed in Table 1. The data were calibrated and imaged using standard routines in the AIPS reduction package.

At 43.3 GHz, the phase center of our map was $\alpha(1950) = 05^h43^m34.9^s$, 6(1950) = –00°11'28.0". The naturally-weighted synthesized beam was 2.6" x 2.4". The only source detected coincides with HH24MMS, at $\alpha(1950) = 05^h43^m34.857^s \pm 0{,}008'$, 6(1950) = –00°11'49.55" ± 0.12". This position was used as the phase center at 14,9 GHz. The three sources detected above a 5σ limit of 275 μJy, II H24MMS, SSV63E, and SSV63W (Lane 1989; Zealey et al. 1989), are all unresolved in the 4.7" x 3.5" naturally-weighted synthesized beam. Their flux densities are listed in Table 2.

We imaged the 88.0 GHz (λ = 3.4 mm) continuum emission from HH24MMS using the 6-element Owens Valley millimeter array on 1995 February 15. The naturally-weighted synthesized beam was 3.0" x 2. l". An average of upper and lower sidebands centered 1.5 GHz either side of 88.0 GHz, with 1 GHz bandwidth and single-sideband system temperature 250 K, gave an rms noise of 1.7 mJy/beam for 1 hour of on-source integration. Atmospheric and instrumental phase was monitored by observing 0528+134 every 15 minutes, The absolute flux density calibration relies on the value for 0528+134 (Table 1) which is based on observations of Uranus and Neptune and is correct to within 20%. The raw visibility data were calibrated using software specific to the Owens Valley array (Scoville et al. 1993), and images were made using AIPS.

Figure 1 shows contour maps of HH24MMS at 43 and 88 GHz. Gaussian fits indicate the emission is resolved at both frequencies, with deconvolved sizes of 1.0" x 0.6" at PA 115° (43 GHz), and 1.4" x 0.7" at PA 85° (88 GHz). Flux densities at each peak and integrated over 7" x 7" boxes centered on HH24MMS are listed in Table 2, However, the 88 GHz visibility amplitudes show both extended emission plus an unresolved component which dominates the source structure for uv-spacings longer than about 40 kλ (Figure 2), Upper limits to the size of the unresolved component are 0.9" (43 GHz) and 1.0" (88 GHz); flux densities obtained by imaging only uv-data longer than 40 kλ and are listed in Table 2.

Figure 3 shows the continuum spectrum of HH24MMS including our new measurements. At 43 and 88 GHz, contributions from the unresolved component are plotted as open circles and from the extended emission as open triangles. At frequencies of 22 GHz and below, the emission is also unresolved; this component can be fitted by a power-law, $F_\nu \propto \nu^{2.68\pm0.12}$, shown as a solid line in Figure 3. Since emission from an ionized wind would have a maximum slope of ν^2 (Reynolds 1986), we conclude that the centimeter-wave emission from HH24MMS originates only from dust,

T.!) ’ er emission from HH24M MS into an unresolved component and
xt consistent with the single power-law intensity profile that would result
?1, id density distributions in an envelope. Instead, it is reminiscent
s around young stars discussed by Terebey et al. (1993), Butner,
Chandler, Carlstrom, & Terebey (1994), Furthermore, the spectral
unresolved component is similar to that derived for disks around T
Sargent 1991). Typically, emission from the envelope dominates at
r wavelengths, while high resolution images at 2.7 mm show mainly
HH24MMS, however, even 7 mm emission is significantly extended,
the envelope detected at 450 μm by Ward-Thompson et al. (1995),

sk

f the unresolved component of $\sim$ 1“ correspond to 400 AU at the 400
on (Anthony -Twarog 1982). For a uniform source 1“ in diameter, a
GHz corresponds to a brightness temperature, T_B, of 10 K; the 88
= 20 K. This is a lower limit to the true dust temperature, and since
velope which can help maint ain high temperatures at large distances
ve adopt T = 100 K (cf. Butner et al. 1994), placing the HH24MMS
e Rayleigh-Jeans part of the Planck curve, Assuming the dust opacity
the centimeter flux densities imply β = 0,68+ 0,12 in the disk.
unresolved component is marginally optically thick at 88 GHz, the
er limit to the value of β of $\leq$ 1.1, This is similar to the value obtained
Sargent 1991; Mannings & Emerson 1994) and somewhat lower than
or the interstellar medium (cf. Emerson 1988). Low values of β have
owth of large dust grains, or changes in grain shape or composition,
Nakagawa 1993; Pollack et al. 1994; Krügel & Siebenmorgen 1994;
If this is the case for HH24MMS, the timescale for changes in the
ties of the dust must be short compared with the infall timescale.
^{12} Hz)$^{\beta}$ c m^2 g^{-1} for the dust mass opacity coefficient, κ_ν (cf. Hilde-
90), the total mass of material in the unresolved component is derived
ugh

$$M = \left(\frac{F_\nu D^2}{\kappa_\nu B_\nu(T)}\right)\left(\frac{\tau_\nu}{1-e^{-\tau_\nu}}\right), \qquad (1)$$

$$^2\left(\frac{\kappa_{10^{12}\ \mathrm{Hz}}}{0.1\ \mathrm{cm^2\ g^{-1}}}\right)^{-1}\left(\frac{\nu}{10^{12}\ \mathrm{Hz}}\right)^{-(3+\beta)}\left(e^{h\nu/kT}-1\right)\left(\frac{\tau_\nu}{1-e^{-\tau_\nu}}\right). \qquad (2)$$

For $T = 20$ K, D = 400 pc and $\beta = 1$, the 88 GHz flux density leads to a mass of $1.8\ \tau_{88}/(1 - e^{-\tau_{88}})\ M_\odot$. If $T \sim 100$ K and $\tau_{88} << 1$, M is much lower, $\sim 0.32 M_\odot$. Taking 0.32 $M_\odot$ as a lower limit to the mass within a radius of 200 AU of the central protostar gives a mean molecular hydrogen number density $\gtrsim 10^9$ c m^{-3}.

3.2 The extended envelope

Our interferometer measurements are insensitive to structure with angular size scales $\gtrsim 10''$ and therefore provide only a lower limit to the contribution to the total 43 and 88 GHz flux densities from an extended component, Any radiative transfer model of the envelope must accommodate flux densities of at least 4 mJy at λ 7 mm and 45 mJy at λ 3.4 mm. In Figure 3 we plot various models that fit the submillimeter points assuming the emission at all wavelengths is optically thin. The models assume temperature distribution $T \propto r^{-2/(4+\beta)}$, *and* density distribution $\rho \propto r^{-3/2}$. For the standard interstellar value of $\beta = 2$ no solution can account for the observed 7 mm flux density. Values for β as high as 1.9 can fit the data as long as all the dust in the envelope is colder than 20 K, otherwise the slope of the spectrum at long wavelengths is too steep, It is difficult to place a lower limit on β in the envelope. The emission throughout the mm/submm has $F_\nu \propto \nu^2$, which can be fitted by any value of β larger than O.

The envelope may not be optically thin at all wavelengths, however. Indeed, for disk temperatures higher than about 40 K the inferred emission at 60 μm exceeds the upper limit measured by Chini et al. (1993), The discrepancy can be explained by an envelope that is optically thick in the far-infrared and obscures the disk emission, A similar situation obtains for the young stellar object L1551-IRS5 (Butner et al. 1994),

Single-temperature fits and detailed radiative transfer modeling lead to an envelope mass, $M_{\rm env}$, of 4-8 $M_\odot$ for HH24MMS (Ward-Thompson et al. 1995), significantly greater than the disk mass. The fraction of the circumstellar mass that resides in the extended envelope is expected to decrease with age (cf. André & Montmerle 1994), confirming that HH24MMS is very young.

4 Conclusions

Images of the protostar HH24MMS at 43 and 88 GHz show the dust emission comprises two distinct components. Most of the long wavelength emission originates from an unresolved disk less than 1" in size, with a spectrum well-fitted over a decade in frequency by a single power-law, $F_\nu \propto \nu^{2.68 \pm 0.12}$ This component accounts for the centimeter emission previously reported by Bontemps et al. (1 995) and Ward-Thompson et al. (1995). The power law spectral index implies a frequency dependence for the dust opacity, β, of 0.68 $\pm$ 0,12, considerably lower than the interstellar value but close to that obtained for circumstellar disks around T Tauri stars (Beckwith & Sargent 1991; Mannings & Emerson 1994; Koerner, Chandler, & Sargent 1995). If this result holds for other young protostars,

the low values of β observed in T Tauri disks cannot be attributed solely to steadily increasing grain growth and planetesimal formation - they may be a feature of any high density environment. Mean densities in excess of $10^9 cm^{-3}$ are derived for the unresolved component.

The second component is the extended envelope first detected at submillimeter wavelengths (Ward-l'hompson et al. 1995). Our interferometer measurements provide firm lower limits to the emission from the envelope at long wavelengths, and show that here β must be less than 1.9. If the fraction of circumstellar material in an extended component compared with a disk decreases with increasing age of the forming star/disk system, HH24MMS must be very young, since the mass of the envelope is an order of magnitude higher than that of the disk.

We thank the referee, Neal Evans, for suggestions which have improved the text. Research at the Owens Valley Radio Observatory is supported by NSF grant AST 9314079. A.I.S. is also supported by NASA grant NAGW 4030, from the "Origins of Solar Systems" program.

'Table 1

Millimeter and centimeter flux densities of quasars

Source	ν (GHz)	F_ν (Jy)	Statistical error (Jy)	Total error (Jy)
0134+329 (3C48)	14.9	1.81*	. . .	...
	43.3	0.53*	. . .	...
1328+307 (3 C286)	43.3	1.47*	. . .	...
0529+075	14.9	?.26	0.02	0.23
0605–085	43.3	2.30	0.05	0.46
0528+1.34	88.0	5.74*	. . .	...

* Assumed value.

Table 2

Millimeter and centimeter flux densities of sources in the HH24 region"

ν (GHz)	Source	F_ν (mJy)	Statistical error (mJy)	Total error (mJy)
14.9	SSV63E	0.36	0.06	0.07
	SSV63W	0.32	0 . 0 6	0.07
	HH24MMS	0.70	0.06	0.09
43.3	Peak	12,3	0.6	2.5
	7" X 7" box	14,5	1.7	3.4
	Unresolved	10.5	0.7	2.2
	Extended	4.0	0.5	1.0
88.0	Peak	108	1.7	22
	7" X 7" box	133	5	27
	Unresolved	88	2	18
	Extended	45	2	9

References

André, P., & Montmerle, T. 1994, ApJ, 420, 837

Anthony -Twarog, B. J. 1982, AJ, 87, 1213

Baars, J. W. M., Genzel, R., Pauliny-Toth, I. I, K., & Witzel, A, 1977, A&A, 61, 99

Beckwith, S. V. W., Sargent, A. I., Chini, R. S., & Güsten, R, 1990, AJ, 99, 924

Beckwith, S. V. W., & Sargent, A. I. 1991, ApJ, 381, 250

Bontemps, S., André, P., & Ward-Thompson, D. 1995, A&A, 297, 98

Butner, H. M., Natta, A., & Evans, N. J. 1994, ApJ, 420, 326

Chandler, C. J., Carlstrom, J. E., & Terebey, S. 1994, in Clouds, Cores, and Low Mass Stars, ed. D. P. Clemens & R. Barvainis, ASP Conf. Ser. 65, 241

Chini, R., Krügel, E., Haslam, C. G. T., Kreysa, E., Lemke, R., Reipurth, B., Sievers, A., & Ward-Thompson, D. 1993, A&A, L5

Emerson, J. P. 1988, in Formation and Evolution of Low Mass Stars, ed. A. K. Dupree & M. T. V. T. Lago, Kluwer, Dordrect, 21

Hildebrand, R. H, 1983, QJRAS, 24, 267

Koerner, D. W., Chandler, C. J., & Sargent, A. I.)995, in preparation

Krügel, E., & Chini, R. 1994, A&A, 287,947

Krügel, E., & Siebenmorgen, R. 1994, A&A, 288,929

Lane, A. P. 1989, in ESO Workshop on Low Mass Star Formation and Pre-Main Sequence Objects, ed. B. Reipurth, ESO, Garching, 331

Mannings, V., & Emerson, J. P. 1994, MNRAS, 267,361

Miyake, K., & Nakagawa, Y. 1993, Icarus, 106,20

Natta, A. 1993, ApJ, 412, 761

Ossenkopf, V., & Henning, T. 1994, A&A, 291,943

Pollack, J. B., Hollenbach, I)., Beckwith, S., Simonelli, D. P., Roush, T., & Fong, W. 1994, ApJ, 421, 615

Reynolds, S. P. 1986, ApJ, 304, 713

Scoville, N. Z., Carlstrom, J, E., Chandler, C. J., Phillips, J. A., Scott, S. L., Tilanus, R. P. J., & Wang, Z. 1993, PASP, 105, 1482

Shu, F., Najita, J., Galli, D., Ostriker, E., & Lizano, S. 1993, in Protostars and Planets III, eds E. H, Levy, S, 1, Lunine, & M. S, Matthews University of Arizona Press, Tucson, 3

Terebey, S., Chandler, C. J., & André, P. 1993, ApJ, 414, 759

Ward-Thompson, D., Chini, R., Krügel, E., André, P., & Bontemps, S. 1995, MNRAS, in press

Zealey, W. J., Mundt, R., Ray, T. P., Sandell, G., Geballe, T., Taylor, K. N, R., Williams, P. M., & Zinnecker, H. 1989, Proc. Astr. Sot. Australia, 8, 62

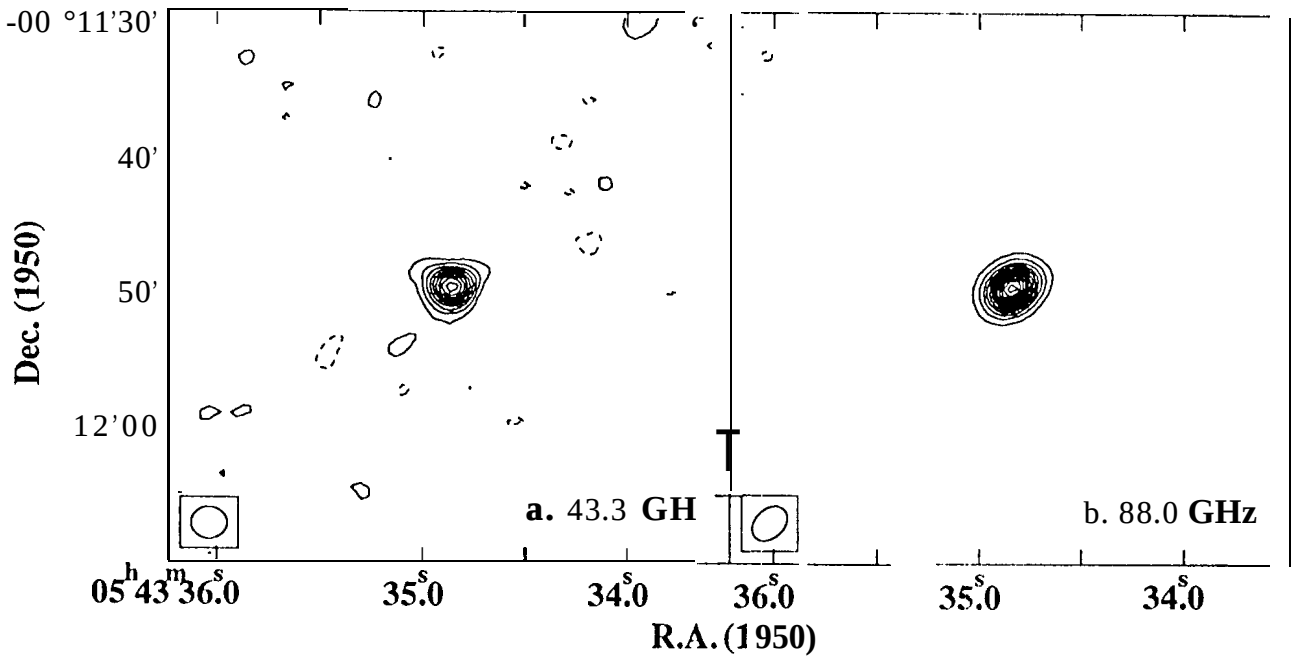

Figure 1. Images of the dust emission from HH 24MMS. (a) 43 GHz image obtained with the VLA. The synthesized beam is 2.6" x 2.4" at P.A. --89°, and the contours are at 2σ intervals of 1.28 mJy/beam beginning at the 2σ level. (b) 88 GHz image obtained with the Owens Valley millimeter array, The synthesized beam is 3.0" x 2,1" at P.A. –44°, and the contours are at 5σ intervals of 8.5 mJy/beam beginning at 8.5 mJy/beam.

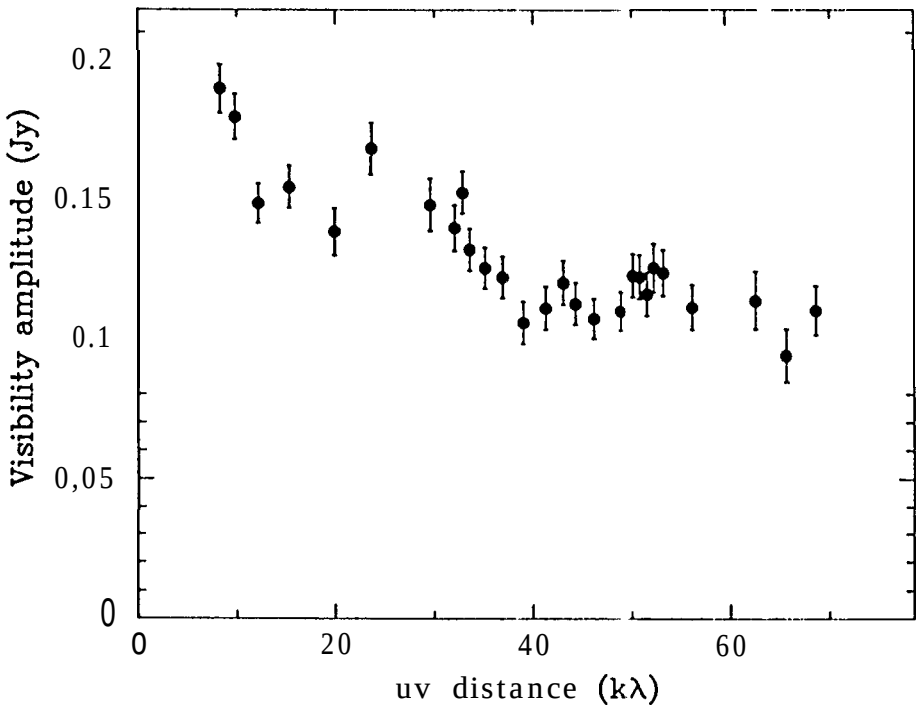

Figure 2. Plot of 88 GHz visibility amplitude vs. *uv*-distance for HH24MMS. At spacings longer than 40 kλ the source structure is dominated by an unresolved component, 'I'he noise associated with measurements of the real and imaginary parts of individual 3-minute risibilities biasses the amplitudes to be higher than their true values.

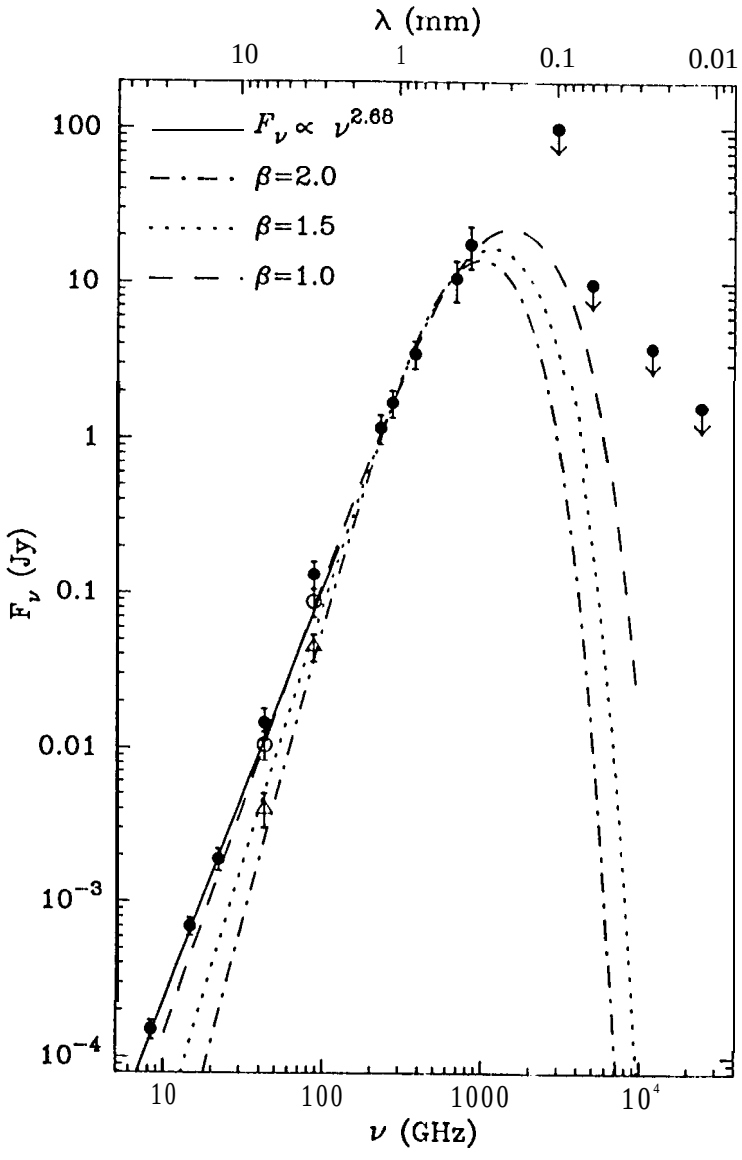

Figure 3. 'l'he dust continuum spectrum of HH24MMS including the IRAS upper limits from Chini et al. (1993), the submillimeter points and the 22 GHz flux density reported by Ward-Thompson et al. (1995), and the 8,4 GHz flux density from Bontemps et al. (1995), all represented by filled circles. At 43 GHz and 88 GHz the contributions to the total flux from the unresolved component are shown as open circles, and from the extended component as open triangles. The solid line is a power-law fit to the radio emission and the unresolved components at 43 GHz and 88 GHz, with $F_\nu \propto \nu^{2.68}$. The other lines are optically-thin fits to the data for an envelope with $T \propto r^{-2/(4+\beta)}$, $\rho \propto r^{-3/2}$, and various values of the dust opacity index β. Dot-dash curve: β = 2.0; dotted curve: $\beta = 1.5$; dashed curve: $\beta = 1.0$. Values of $\beta \geq 1.9$ cannot fit the submillimeter points and account for the extended components at 43 GHz and 88 GHz.